

Static and dynamical disorder of NiCl₂ clusters intercalated in graphite

G. Faraci, S. La Rosa, and A. R. Pennisi

*Dipartimento di Fisica, Università di Catania, Gruppo Nazionale di Struttura della Materia,
Consorzio Interuniversitario di Fisica della Materia, Corso Italia 57, 95129 Catania, Italy*

S. Mobilio

*Dipartimento di Energetica, Università dell'Aquila, Roio Montelucio, 67100 L'Aquila, Italy,
and Istituto Nazionale di Fisica Nucleare, Laboratori Nazionali di Frascati, 00044 Frascati, Italy*

I. Pollini

*Dipartimento di Fisica-Università di Milano, Gruppo Nazionale di Struttura della Materia,
Consorzio Interuniversitario di Fisica della Materia, via Celoria 16, 20133 Milano, Italy*

(Received 4 March 1991; revised manuscript received 5 November 1991)

We report an experimental study on static and dynamical disorder of nickel dichloride intercalated in graphite, by means of extended x-ray-absorption fine-structure measurements on the Ni *K* edge at different temperatures. As we have shown in a previous paper, at room temperature the NiCl₂ molecules are intercalated between the hexagonal planes of graphite in the form of clusters or islands without significant short-range distortion. However, the question remained unsolved if the graphite lattice can induce a structural distortion of the Cl positions such that the disorder is increased but the Ni-Cl average distance is unchanged. Our present results, performed at low temperature, confirm our previous data of the interatomic distances but indicate that the NiCl₂ molecule undergoes a static deformation upon intercalation. The dynamical properties of the nickel dichloride clusters measured by the behavior of Debye-Waller factors versus temperature show the same trend as the crystal in the first shell but indicate the presence of a softening of the second-shell bond due to the clustering.

I. INTRODUCTION

Graphite intercalation compounds (GIC) represent an interesting class of lamellar materials showing a series of peculiar properties already outlined in many papers.¹⁻⁸ These layered structures are formed² by inserting atomic or molecular layers of different chemical species between the hexagonal layers of the graphite lattice.

In a previous paper¹ the structural and vibrational properties of NiCl₂-GIC have been investigated at room temperature by a comparison with the properties of the single crystal, using extended x-ray-absorption fine-structure (EXAFS) spectroscopy. It was shown that the NiCl₂ molecules intercalate between the graphite planes as small clusters with a small short-range distortion with respect to the parent material. An increase of the absolute mean-square fluctuations of the Ni-Cl first-shell distance of the intercalant with respect to the crystal was evidenced by a relevant increase of the Debye-Waller factor. Such an effect was rather small on the Ni-Ni second-shell distance. The interpretation of these results was not unequivocal, on the basis of room-temperature spectra only, and two possible explanations were advanced. The first attributed the increase of the Debye-Waller factor to the softening of the lattice in the intercalation compound due to the lack of three-dimensional periodicity. In the second interpretation, the incommensurate graphite lattice induces distortions in the position of Cl atoms, increasing the fluctuation of the Ni-Cl

distances, but leaving their average values almost unchanged. In both explanations the second-shell (Ni-Ni) disorder is expected to be quite small.

It is possible to discriminate between the two previous explanations by analyzing the temperature dependence of the Debye-Waller factors of the intercalated compound, with respect to the pristine parent material. In fact, at low temperature the static disorder is predominant with only a small contribution due to the lattice zero-point vibrational energy, while the increase with the temperature of the Debye-Waller factor is governed by the dynamical interaction between nearest neighbors: a hardening or softening of the lattice appears when the binding forces increase or decrease, respectively.

In this paper we analyze the thermal behavior of the Debye-Waller factors in NiCl₂-GIC, separating the static and dynamical contribution of the Debye-Waller factor.

II. EXPERIMENT

The EXAFS spectra were obtained for the Ni *K* edge in the range 8250-9200 eV using the fluorescence-detection scheme. As NiCl₂ is hygroscopic, commercial samples can contain a small percentage of contaminants like oxygen or water due to long storage or improper handling. Therefore we prepared our own sample. Single crystals of NiCl₂ were obtained from the vapor phase by the dynamical transport method at temperatures around 700 °C. Chlorine gas was passed through a quartz pipe,

where the reaction occurred. The large crystals obtained were stored in vacuum; surface layers were peeled off immediately before the measurements.

The intercalated samples purchased from Alfa Products Company in powder form were handled under dry argon. The stage of our GIC is not known; it was, however quite high, since the dilution of the chloride molecule into the graphite corresponds to about 20%. The experiment was performed at the PULS facility of Frascati National Laboratory using the radiation emitted from a bending magnet with a critical energy of 1.5 keV. The radiation was monochromated by a Si(111) channel-cut crystal, and the intensity of the monochromatic radiation was monitored by using an ion chamber. The average photon flux was 10^9 photons/s and the resolution about 2 eV. The intensity of the fluorescent radiation was measured by a NaI(Tl) detector. During the measurements the sample was under vacuum; the spectra were recorded at 60, 120, 180, 240, and 300 K for both the reference compound and for the GIC sample. Several measurements have been collected on each sample to check for reproducibility and to increase the signal-to-noise ratio. No effect was detected for different orientations either of the crystal sample or of the intercalated GIC.

III. RESULTS AND DISCUSSION

The normalized fluorescence spectra I_F/I_0 were analyzed according to standard procedures.⁹ The EXAFS oscillations were extracted fitting the absorption coefficient with a polynomial curve, in the k range 2–13 \AA^{-1} above the absorption edge.

Well-known EXAFS spectra are represented by¹⁰

$$\chi(k) = \sum_i \frac{N_i S_0^2(k) F_i(k)}{k r_i^2} e^{-2\sigma_r^2 k^2} e^{-2(r_i - \Delta)/\lambda} \times \sin[2kr_i + \phi_i(k)]$$

with the usual meanings of the symbols. The technique gives valuable information on the structural properties as interatomic distances and coordination numbers as well as on the Debye-Waller factors σ_r^2 , which give the mean-square fluctuations of the shell at distance r_i from the absorbing atom. The previous formula includes also amplitude attenuation due to many-body effects,¹⁰ inelastic losses, and lifetime effects. For a detailed discussion the reader is referred to the literature¹¹ and to our previous paper.¹ We shall limit ourselves to analyzing the behavior of the Debye-Waller factor as a function of the temperature, since the structural properties of the intercalated compound compared to the crystalline lattice have already been published.¹

We confirm here our previous conclusions about the presence of a very small distortion of the NiCl_2 -GIC molecule. In fact, as reported in Ref. 1, the first-shell (Ni-Cl) distance shows in the GIC a negligible contraction with respect to the crystal within the experimental uncertainty. This implies that the average atomic position is unchanged, since in the Fourier transform of the EXAFS

spectra at any temperature the first-shell peak did not show any shift or separation in two or more components with respect to the crystal. However, the broadening of the peak related to the Debye-Waller factor as a function of the temperature allows us to ascertain if there is a static deformation even if the atomic average position is unchanged. Further, the unchanged coordination number of the first shell, together with the reduction to about one-half of the second-shell coordination number, implies a clusterization process of the NiCl_2 upon intercalation.

Before presenting our results, we recall that in the fluorescence-detection scheme the normalized experimental spectra I_F/I_0 are proportional to the absorption coefficient only in the two extreme cases of thin samples and diluted samples. In our case both samples were thick and concentrated, therefore the experimental spectra present an attenuation in the amplitude of the EXAFS oscillations.¹² This attenuation does not influence the evaluation of the distances for which only the phases of the oscillations are relevant, but must be carefully taken into account for an evaluation of the coordination numbers and of the Debye-Waller factors. To evaluate this effect we have used the same procedure already described in Ref. 1.

In Fig. 1 the EXAFS spectra measured on the crystal and on the NiCl_2 -GIC are reported at three temperatures (300, 180, and 60 K). Similar results were obtained also at 240 and 120 K. All the spectra have been Fourier transformed, to obtain in real space peaks that correspond to the different shells. Then the contribution to the first Ni-Cl and second-shell Ni-Ni was extracted and backtransformed.

From the inverse Fourier transforms of each shell we

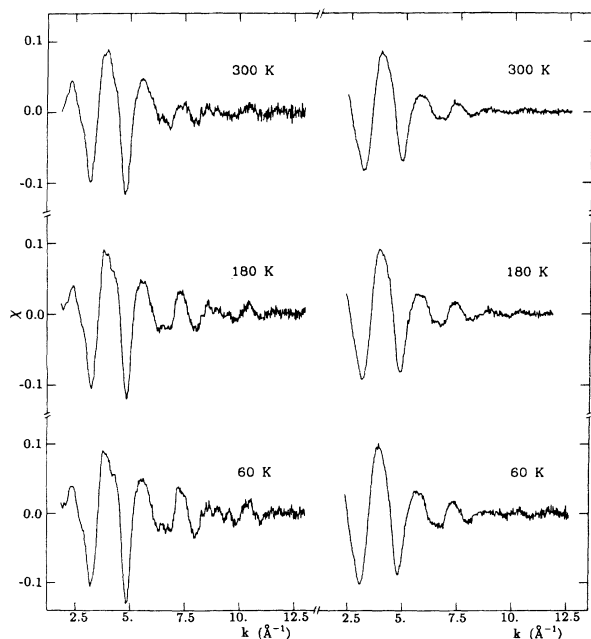


FIG. 1. Spectra $\chi(k)$, obtained on the Ni K edge at the temperature specified. On the left-hand side are the crystalline spectra, on the right the GIC spectra.

TABLE I. For both NiCl₂ single crystal and NiCl₂-GIC samples. Relative Debye-Waller factor for the first-shell Ni-Cl.

| T (K) | Crystal | GIC |
|-------|--|--|
| | $\sigma_T^2 - \sigma_{60\text{K}}^2$ (Å ²) | $\sigma_T^2 - \sigma_{60\text{K}}^2$ (Å ²) |
| 300 | 0.0051±0.0005 | 0.0039±0.0005 |
| 240 | 0.0025±0.0005 | 0.0034±0.0005 |
| 180 | 0.0015±0.0003 | 0.0019±0.0003 |
| 120 | 0.0006±0.0002 | 0.0007±0.0002 |

derived the relative Debye-Waller factor

$$\Delta\sigma^2 = \sigma^2(T) - \sigma^2(T_0)$$

plotting the function

$$\ln[\chi(k, T)/\chi(k, T_0)] = -2k^2\Delta\sigma^2$$

versus k^2 . In the above expressions T_0 is the temperature of the reference spectrum. Such a plot gives a straight line with a slope related to the relative Debye-Waller factor $\Delta\sigma^2$. The spectrum taken at the lowest temperature, 60 K, was used as reference. Results so obtained are shown in Table I for the first coordination shell. They show a behavior versus temperature quite similar in the two samples, indicating that the two materials have similar dynamical properties.

From the previous spectra it is possible to make a further comparison: in order to investigate the static behavior of the GIC Debye-Waller factor we have compared at the same temperature the spectra of the GIC and the spectra of the crystal, obtaining the differences $(\sigma_{\text{GIC}}^2 - \sigma_{\text{cry}}^2)_T$ reported in Table II. It is clear that at any temperature the intercalated compound has a Debye-Waller factor larger than the crystal as much as about 0.006 Å². This supports the second of the two previously indicated models, confirming the idea that the static disorder of the GIC increases upon intercalations as the to-

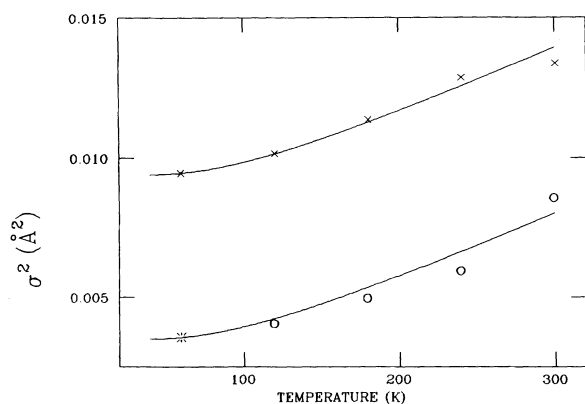


FIG. 2. Debye-Waller experimental data for the first shell: ○, crystal values; ×, GIC values. The crystal data have been obtained by the values reported in Table I, adding the calculated reference value $\sigma^2(T=60\text{ K})$ shown in the plot by an asterisk. The GIC data have been obtained by the values reported in Table I, adding the relative displacement reported in Table II. The solid lines are the fits obtained by means of the Einstein approximation.

TABLE II. Relative Debye-Waller factor, at the specified temperature, between the GIC and the crystal for the first-shell Ni-Cl.

| T (K) | $\sigma_{\text{GIC}}^2 - \sigma_{\text{cry}}^2$ (Å ²) |
|-------|---|
| 300 | 0.0046±0.0005 |
| 240 | 0.0070±0.0005 |
| 180 | 0.0065±0.0003 |
| 120 | 0.0058±0.0002 |
| 60 | 0.0059±0.0002 |

poloical configuration of the clusters in the GIC implies only short-range binding forces with asymmetrical arrangement due either to the graphite atoms surrounding the clusters or to the lack of three-dimensional periodicity of the molecule.

To get the *absolute* mean-square vibrational displacement at a given temperature it is necessary to find out the reference value $\sigma^2(T_0)$. As shown in Refs. 13 and 14, for a monoatomic crystal in the harmonic approximation the single-shell mean-square fluctuations σ_R^2 can be written as

$$\sigma_R^2 = (\hbar/M) \int d\omega \rho_R(\omega) \frac{\coth(\beta\hbar\omega/2)}{\omega}, \quad (1)$$

where M is the atomic mass, $\beta = 1/kT$. $\rho_R(\omega)$ is the normalized projected density of modes contributing to the relative vibrational motion and can be calculated in the Debye or in the Einstein approximation. In this last approach,

$$\sigma_R^2 = \sigma_0^2 \coth(\Theta_E/2T), \quad (2)$$

where ω_E is the Einstein frequency, Θ_E the Einstein temperature: $\Theta_E = \hbar\omega_E/k$, and $\sigma_0^2 = (\hbar/M\omega_E)$.

The system we are studying is highly asymmetric and polyatomic, therefore the previous expressions do not hold accurately. However, it has been shown¹⁰ that for many dichlorides of transition metals the Einstein approximation works quite nicely. We thus have adopted the following expression:

$$\sigma_R^2(T) - \sigma_R^2(T_0) = \sigma_0^2 [\coth(\Theta_E/2T) - \coth(\Theta_E/2T_0)] \quad (3)$$

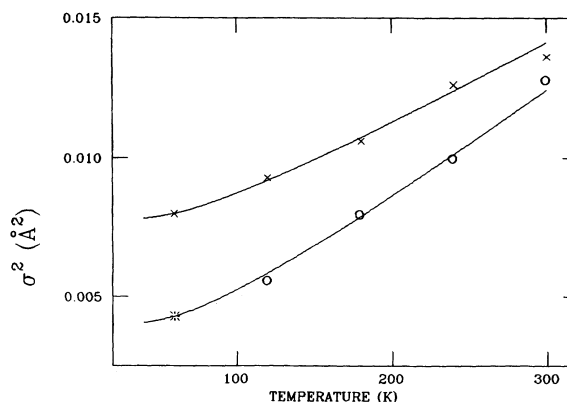


FIG. 3. Analogous to Fig. 2 for the second-shell Ni-Ni.

to fit the data of Table I and get the parameters σ_0^2 and Θ_E . From the fit we obtained, within the experimental uncertainty, the same values both for the crystal and for the GIC: $\sigma_0^2 = 3.5 \times 10^{-3} \text{ \AA}^2$, $\Theta_E = 280 \text{ K}$. We note that for NiCl_2 single-crystal these values are in excellent agreement with the data of Ref. 10 for similar compounds.

In the lower part of Fig. 2 we plot Eq. (3) together with the experimental values of Table I for the NiCl_2 single crystal, shifted by the calculated value σ^2 ($T = 60 \text{ K}$). In the same figure the data of the GIC sample are also reported, shifted from the crystal values by the relative displacement reported in Table II. It can be observed that the agreement between the fits and experimental values is very satisfactory.

A similar data treatment was performed for the second shell and the results are summarized in Tables III and IV, and in Fig. 3. The fits of the data of Table III, according to the formula (3), gave for the second shell the following values:

$$\text{crystal: } \sigma_0^2 = 4.0 \times 10^{-3} \text{ \AA}^2, \quad \Theta_E = 200 \text{ K},$$

$$\text{GIC: } \sigma_0^2 = 3.0 \times 10^{-3} \text{ \AA}^2, \quad \Theta_E = 200 \text{ K}.$$

It is worth noting that for this second shell the value σ_0^2 is not the same for the crystal as for the GIC. This is due to the fact that the value of σ_0^2 reflects the effective mass of the interacting couple (Ni-Ni) and this is modified by the different binding due to clustering in the GIC sample. The reduced coordination of the second shell in the GIC clusters implies in fact a softening of the lattice as reflected by the reduced zero-point vibrational amplitude due to the modification of the effective reduced mass.

Further, for this shell the Einstein temperature is unchanged between the crystal and the GIC with a value (200 K) quite lower than the figure obtained for the first shell (280 K); this is because in the Einstein model the distance of the interacting couples is related to the wavelength of the vibrations: the second shell, at higher distance, vibrates at a main frequency lower than the first shell. This is reflected by the value of Θ_E . No change is detected for the Einstein temperature of GIC with respect to the crystal as the second-shell distance is the same for the two configurations.

Let us compare now Figs. 2 and 3. For the crystal the conclusion that the absolute mean-square displacements at any temperature are, as expected, lower for the first shell than for the second one is evident. Moreover, the dynamical behavior is somewhat different because of the change in the atomic effective mass (which enters the σ_0^2)

TABLE III. Same as for Table I for the second-shell Ni-Ni.

| T (K) | Crystal | GIC |
|---------|---|---|
| | $\sigma_T^2 - \sigma_{60 \text{ K}}^2$ (\AA^2) | $\sigma_T^2 - \sigma_{60 \text{ K}}^2$ (\AA^2) |
| 300 | 0.0086 ± 0.0005 | 0.0056 ± 0.0005 |
| 240 | 0.0058 ± 0.0005 | 0.0046 ± 0.0005 |
| 180 | 0.0038 ± 0.0003 | 0.0026 ± 0.0003 |
| 120 | 0.0014 ± 0.0002 | 0.0012 ± 0.0002 |

TABLE IV. Same as for Table II for the second-shell Ni-Ni. Also reported is the relative coordination for this second shell.

| T (K) | $\sigma_{\text{GIC}}^2 - \sigma_{\text{cry}}^2$ (\AA^2) | $N_{\text{GIC}}/N_{\text{cry}}$ |
|---------|--|---------------------------------|
| 300 | 0.0007 ± 0.0005 | 0.45 ± 0.05 |
| 240 | 0.0025 ± 0.0005 | 0.42 ± 0.05 |
| 180 | 0.0026 ± 0.0003 | 0.52 ± 0.03 |
| 120 | 0.0036 ± 0.0002 | 0.47 ± 0.02 |
| 60 | 0.0038 ± 0.0002 | 0.52 ± 0.02 |

and in the Einstein temperature which reflects the main optical frequency of the vibrations. This is related to the binding force constants of the coupling Ni-Cl for the first shell and Ni-Ni for the second one.

In the intercalation compound the enlarged contribution to the static value with respect to the crystal is due to the distortion of the intercalated molecule. In Fig. 3 the different thermal behavior of the second-shell Debye-Waller factors is clearly visible. We ascribe it to the reduced coordination of the Ni-Ni bond in the GIC sample, which produces a softening of the lattice. In Table IV we have also reported the coordination number of the Ni-Ni pairs in the GIC sample with respect to the NiCl_2 crystal. A value around 0.5 is found, due to the already mentioned clustering of the NiCl_2 in the layered sample.

As a further check of the data obtained for the crystals we have evaluated in the Debye approximation the absolute mean-square fluctuations introducing into Eq. (1) the total phonon density calculated in Ref. 8 and reported in Fig. 4. The effective masses of the couple Ni-Cl or Ni-Ni were evaluated from the asymptotic values of σ_0^2 .

This procedure is, of course, a raw approximation because the projected density of modes would be necessary for a correct calculation of the Debye-Waller factors for the first and second shells. However, we performed the integral between integration limits that take into account the peculiar differences between the modes contributing to the two shells as discussed before: in particular, the low-frequency mode corresponding to the first peak of Fig. 4 was not included for the first shell. Accordingly,

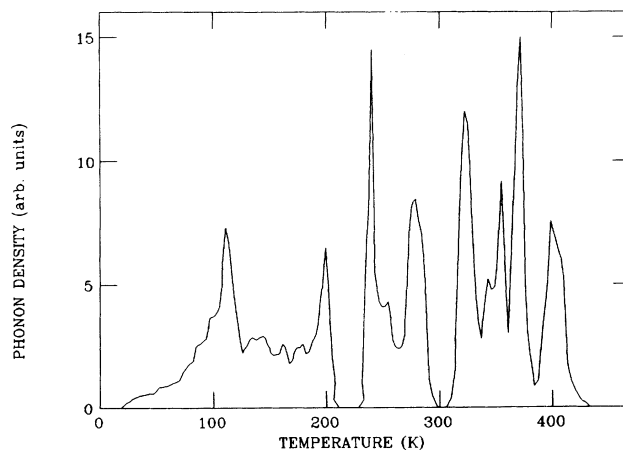


FIG. 4. Phonon frequency density of the NiCl_2 crystal as calculated in Ref. 8. The abscissa of Ref. 8 has been converted to temperature scale ($\hbar\omega = kT$).

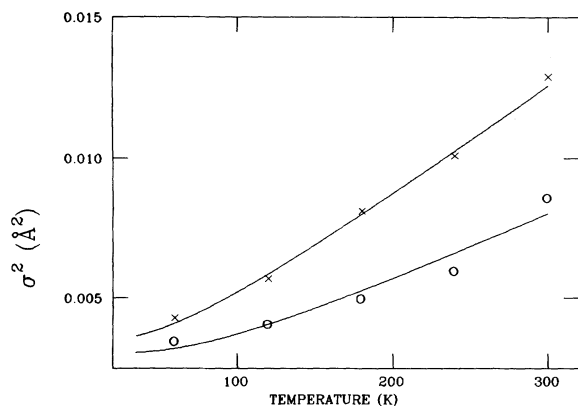


FIG. 5. Lower curve: calculated Debye curve for the first shell of the NiCl₂ crystal according to formula (1) and using the integration limits specified in the text. The points are the experimental data. Upper curve: same as the lower curve, but for the second shell of the crystal.

the integration limits for the first shell correspond to 130–460 K, and for the second shell to 80–460 K.

The plots of these calculated values are reported in Fig. 5, together with our measured data. As can be seen, the agreement is fairly good, confirming that a Debye model reproduces also quite nicely the temperature dependence of the vibrational behavior of these compounds.

In conclusion, we have separated the static and the dynamical contribution to the disorder in graphite intercalated molecules. We have shown that an increase in the static disorder is present due to the distortion of the NiCl₂ molecules induced by the intercalation in graphite. The clustering of the NiCl₂ molecules does not change the short-range forces, but gives rise to a softening of the long-range forces.

ACKNOWLEDGMENTS

We would like to thank the ADONE machine staff of the Laboratori Nazionali di Frascati, and in particular N. Campolungo for his constant technical assistance.

- ¹G. Faraci, S. La Rosa, A. R. Pennisi, S. Mobilio, and I. Pollini, *Phys. Rev. B* **43**, 1913 (1991).
²M. S. Dresselhaus and G. Dresselhaus, *Adv. Phys.* **30**, 139 (1981), and references therein.
³L. Pietronero and S. Straessler, *Phys. Rev. Lett.* **47**, 593 (1981).
⁴Masatsugu Suzuki and Hironobu Ikeda, *J. Phys. C* **14**, L923 (1981).
⁵D. G. Rancourt, C. Meshi, and A. Flandrois, *Phys. Rev. B* **33**, 347 (1986).
⁶S. Flandrois, A. W. Hewat, C. Hauw, and R. H. Bragg, *Synth. Met.* **7**, 305 (1983).
⁷D. J. Lockwood, D. Bertrand, P. Carrara, G. Mischler, D. Billerey, and C. Terrier, *J. Phys. C* **12**, 3615 (1979).

- ⁸G. Benedek and A. Frey, *Phys. Rev. B* **21**, 2482 (1980).
⁹P. A. Lee, P. H. Citrin, P. Eisenberg, and B. M. Kincaid, *Rev. Mod. Phys.* **53**, 769 (1981).
¹⁰E. A. Stern, B. A. Bunker, and S. M. Heald, *Phys. Rev. B* **21**, 5521 (1980).
¹¹B. Lengeler and P. Eisenberger, *Phys. Rev. B* **21**, 4507 (1980); G. Faraci, A. R. Pennisi, A. Terrasi, and S. Mobilio, *ibid.* **38**, 13 468 (1988).
¹²Z. Tan, J. I. Budnik, and S. M. Heald, *Rev. Sci. Instrum.* **60**, 1021 (1989).
¹³G. Beni and P. M. Platzman, *Phys. Rev. B* **14**, 1514 (1976).
¹⁴E. Sevillano, H. Meuth, and J. J. Rehr, *Phys. Rev. B* **20**, 4908 (1979).